Sobell, H. M. (1973) *Prog. Nucleic Acid Res. Mol. Biol. 13*, 153–190.
Suck, D., Lahm, A., & Oefner, C. (1988) *Nature 382*, 465–468.
van Dyke, M. W., Hertzberg, R. P., & Dervan, P. B. (1982) *Proc. Natl. Acad. Sci. U.S.A. 79*, 5470–5474.
Ward, B., Rehfuss, R., Goodisman, J., & Dabrowiak, J. C. (1988) *Nucleic Acids Res. 16*, 1359–1369.

Structural Changes and Enhancements in DNase I Footprinting Experiments†

Jerry Goodisman* and James C. Dabrowiak*
Department of Chemistry, Room 1-014, Center for Science and Technology, Syracuse University, Syracuse, New York 13244-4100

Received March 28, 1991; Revised Manuscript Received September 17, 1991

ABSTRACT: In footprinting experiments, an increase in DNA cleavage with addition of ligand to a system may be due to a ligand-induced structural change. Ligand binding also enhances cleavage by displacing the cleavage agent from ligand-binding sites, thus increasing its concentration elsewhere. The theory and characteristics of this mass-action enhancement are given, and it is shown how it may be recognized. Results of DNase I footprinting of small oligomers, with actinomycin D as ligand, are analyzed to reveal which enhancements are due to mass action, and which can reasonably be ascribed to structural changes. Patterns in the footprinting plots from our experiments on actinomycin D binding to a 139-base-pair DNA fragment (with DNase I as a probe) are studied in the same way. The likely origins of these patterns are discussed, as are enhancements occurring with other probes commonly used in footprinting experiments.

The binding of drugs and other ligands may induce structural changes in DNA, which may be detected by a number of techniques. Since the rate of cleavage at a particular bond by agents such as DNase I depends on the local DNA structure (Lomonosoff et al., 1981; Drew, 1984; Suck et al., 1988), a natural way to study such changes is the footprinting technique. In a footprinting experiment, one measures the amounts of DNA fragments of different lengths produced by a cleavage agent, and hence the amount of cutting taking place at various positions on a DNA oligomer, as a function of the ligand concentration (Dabrowiak & Goodisman, 1989; Dabrowiak et al., 1991). The amount of cutting at positions at or near ligand binding sites on DNA will decrease with ligand concentration because the bound ligand prevents the approach of the cleavage agent (inhibition), but, at other positions, one might expect to see changes in cutting rate due to structural changes in the DNA. It should be noted that ligand-induced structural changes may lead to *increases* or *decreases* in the observed cutting rate. Thus, Low et al. (1984) observed large enhancements in cutting by DNase I and DNase II at many sites on a 160-base-pair DNA fragment when echinomycin was allowed to bind, in addition to inhibition of cutting near the drug binding sites (having the sequence CpG). These authors noted two possible explanations for the enhancements: structural changes in DNA and an attractive interaction between the cleaving protein and the antibiotic, leading to increased concentration of the former near antibiotic-binding sites. They were able to dismiss the latter explanation.

However, it is now clear (Ward et al., 1988; Dabrowiak & Goodisman, 1989; Dabrowiak et al., 1991; Portugal, 1989) that there is a third explanation for rate enhancements in DNase I footprinting experiments. Increased cutting at sites where no ligand binds can arise from a mass-action effect, caused by the bound ligand displacing the cleavage agent away from some regions of DNA, and thus increasing the concentration of cleavage agent elsewhere. This means that one may not automatically interpret cleavage rate enhancements as ligand-induced structural changes, since the mass-action effect, due to the equilibrium between DNase I and DNA, is always present. Since mass-action and structural effects may exist simultaneously (Portugal, 1989; Ward et al., 1988), one must always consider whether observed enhancements can be explained by mass action alone or if they are the result of a structural change as well.

Below, we give a model for the mass-action enhancement and discuss how one can judge whether enhancements observed in a footprinting experiment have a structural origin. Then, we consider observed enhancements on small DNA oligomers and longer fragments, previously noted by other workers, which may be due to structural changes or mass-action effects. The experimentally observed intensity enhancements for actinomycin D interacting with a 139-mer that we believe to be structural in origin are then presented and discussed.

Experimental Procedures

The quantitative footprinting studies involving actinomycin D, the 139-base-pair *Hin*dIII/*Nci*I restriction fragment of pBR 322 DNA, and DNase I were as earlier described (Ward et al., 1988). The sequence of the restriction fragment and the location of strong and weak actinomycin D binding sites are shown in Figure 1. Autoradiographic spot intensities, corresponding to relative amounts of 54 cleavage products of different lengths, were measured for 26 actinomycin D concentrations ranging from 0 to 38.8 μM.

The model used to interpret the resulting footprinting plots, plots of spot intensity as a function of total drug concentration, is described in detail elsewhere (Goodisman et al., 1992). The analysis takes into account binding of drug at the various binding sites, the mass-action enhancement, and binding of the drug to unlabeled carrier DNA (calf thymus). Correct description of the carrier, described as a concentration of strong binding sites and a concentration of weak binding sites, is important, since it is mainly the equilibria between drug and

† We ackowledge the American Cancer Society, Grant NP-681, for supporting this research.

0006-2960/92/0431-1058$03.00/0

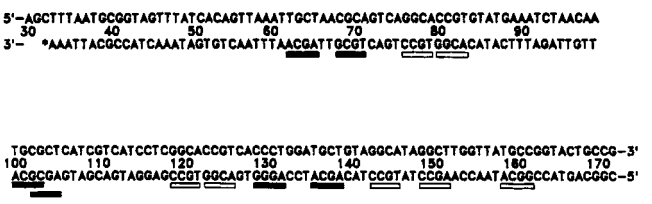

FIGURE 1: Sequence of the 139-base-pair restriction fragment used for DNase I footprinting experiments, with actinomycin D as ligand. Filled rectangles show the location of strong actinomycin D binding sites while the unfilled reactangles indicate weak sites.

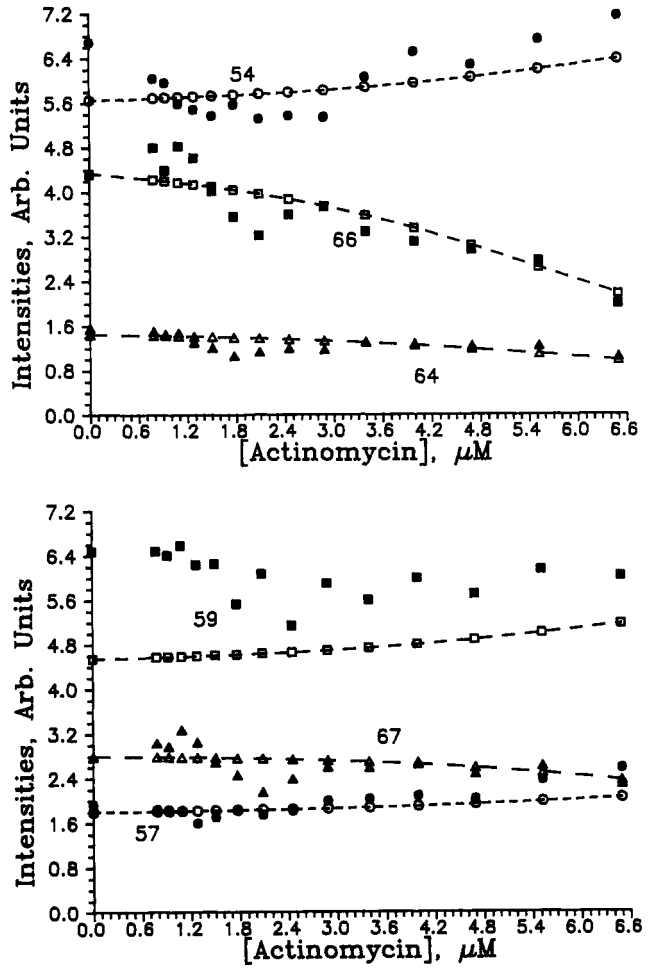

FIGURE 2: Footprinting plots for several sites on the 139-mer for low drug concentrations. Experimental intensities are shown as solid symbols; intensities calculated from a model including drug-binding and mass-action effects are shown as open symbols and broken lines. The pattern of interest is located at ~1.8 μM.

carrier sites that determine the free-drug concentration present in the system. Parameters in the model, such as binding constants, were determined to minimize D, the mean-square deviation between experimental and calculated spot intensities. Although the value of D was of the same size as that of the apparent experimental error in the intensities, some systematic deviations between experimental and calculated footprinting plots were noted which may indicate structural changes.

Figure 2 shows part of the footprinting plots (intensities for 15 drug concentrations below 6.6 μM) for six cutting sites. Measured intensities are plotted as solid symbols; intensities calculated from the model with the best values of the parameters are plotted as open symbols. In Figure 3, the full footprinting plots for eight other cutting sites are displayed with calculated intensities plotted as broken curves. We will be concerned later with two patterns: one at low drug concentrations and one near the 20 μM drug concentration.

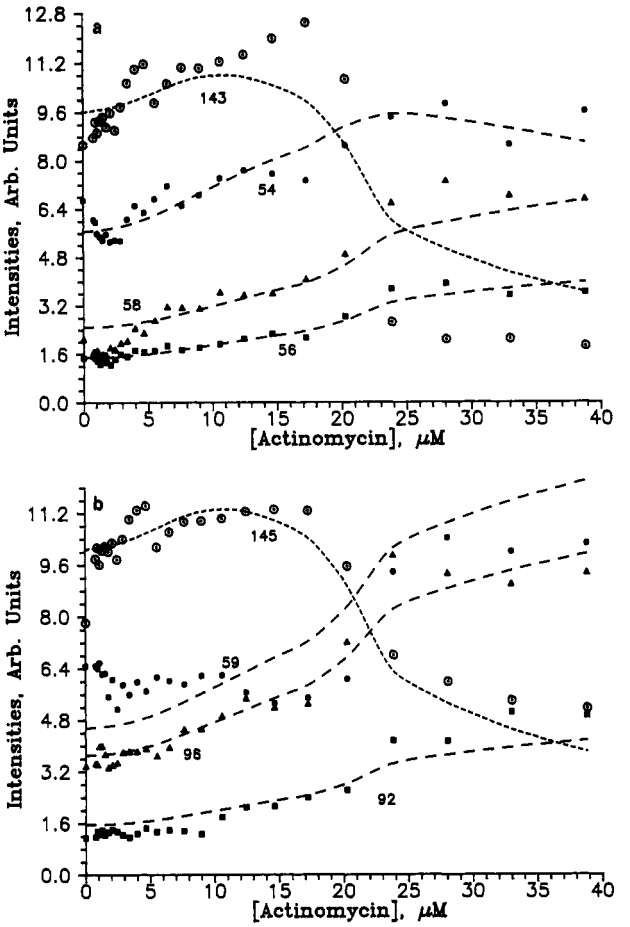

FIGURE 3: (a) Footprinting plots for 54, 56, 58, and 143 on the 139-mer. Sites 54, 56, and 58 exhibit a sudden increase in intensity at ~20 μM while site 143 exhibits a sudden decrease. (b) Footprinting plots for sites 59, 92, 96, and 145 on the 139-mer. Sites 59, 92, and 96 show sudden increases in intensity at ~20 μM while site 145 shows a decrease. Theoretically calculated footprinting plots are shown as a broken line.

The first is a slight (about 10%) decrease, followed by an increase, in intensity, with a minimum for a total drug concentration of about 2 μM. It is seen most clearly on the footprinting plots for sites 52–56, 80–83, 89, and 90, which do not show drug binding, but the pattern seems also to be present, superposed on the intensity decrease due to drug binding, on the plots for these sites: 62–64, 68, 69, 75–81, 83, 87, 92, 114, 120. The site number refers to the sequence shown in Figure 1. Scatter in the experimental intensity data for other sites makes it impossible to state whether this pattern is present there. By classifying all sites as positive, negative, or uncertain, we may summarize the situation by saying that sites from 54 to 103, in a well-resolved region of the autoradiogram, are either positive or uncertain and that sites from 103 to 161, in a poorly resolved region, are either negative or uncertain.

Another noticeable pattern occurs for total drug concentration between 16 and 24 μM. In this concentration range, the shapes of a number of footprinting plots change abruptly, with intensities showing a sharp increase or a sharp decrease with drug concentration. This results in a drop in the total cut of almost 25% at total drug concentration of about 20 μM. In general, binding-type plots show a decrease in intensity in this range and enhancement-type plots show an increase. Since footprinting plots for bonds blocked by drug binding to strong drug sites have very low intensities for a total drug concen-

tration of 16 μM, it is impossible to state whether they show this change in intensity, as is true for other low-intensity footprinting plots. Also, scatter in the experimental intensities may obscure the intensity changes we are looking for in some cases and give the impression of abrupt change when none is actually present in others. With these cautions, we find abrupt intensity increases in the following enhancement plots: 54, 55, 56, 57, 58, 59, 90, 92, 94, 95, 96, 108, 126, 150. Weak-binding plots with abrupt intensity decreases are 71, 75, 76, 77, 78, 79, 80, 83, 89, 99, 114, 120, 124, 143, 145, 154, and 158. Plots for which intensities are high, but show no abrupt changes, are 85, 87, 98, 106, 112, 128, 147, 158, and 161.

THEORY

Mass-Action Enhancement. The cleavage rate, and hence the amount of cleavage, at any bond i of a DNA polymer is proportional to the local concentration of cleavage agent or probe, c_{pi}, and the probability that bond i is not blocked by bound ligand, ν_i. Thus

$$(\text{rate})_i = k_i' c_{pi} \nu_i \tag{1}$$

Structural effects change $(\text{rate})_i$ by changing the rate constant k_i'. The mass-action effect increases $(\text{rate})_i$ by increasing c_{pi} by a factor which is the same for all bonds i. Presence of ligand-induced structural changes in DNA could increase or decrease k_i' by different amounts for different bonds i.

The amount of cleavage at any bond of a DNA oligomer is proportional to the local concentration of cleavage agent or probe, which is determined by equilibria between unbound or free probe and probe bound on DNA at the bond. If the binding constant for probe is much less than the binding constant for a ligand, binding of a ligand will always displace a bound probe molecule. If the ligand binds only at certain sites on DNA, and the probe can bind (and cut) at many sites, the effect of ligand binding is to reduce the number of sites available for probe binding. The competition between ligand and probe takes place on the carrier DNA, if it is present, as well as on the radiolabeled fragment. Since carriers are generally in much higher concentration than the radiolabeled fragment, it is the equilibrium with carrier DNA that determines the free-drug and free-probe concentrations present in the system.

Let c be the total concentration of probe-binding sites, on the carrier and on the fragment. For simplicity, we consider that all of these sites have the same equilibrium binding constant, K, where

$$K = c_p/(c - c_p)(p_t - c_p) \tag{2}$$

with c_p the concentration of bound probe and p_t the total probe concentration. The concentration of probe at any site is proportional to c_p/c. The equilibrium equation (eq 2) is easily solved to give

$$c_p = \tfrac{1}{2}[p_t + c + K^{-1} - ((p_t + c + K^{-1})^2 - 4cp_t)^{1/2}]$$

If the ligand blocks a fraction $(1 - f)$ of the probe sites, the concentration of available sites is reduced to fc. The equilibrium is as in eq 2 except that fc is substituted for c and the concentration of bound probe in the presence of ligand is

$$c_{pf} = \tfrac{1}{2}[p_t + fc + K^{-1} - ((p_t + fc + K^{-1})^2 - 4fcp_t)^{1/2}]$$

The enhancement factor is the ratio of local concentrations, given by

$$E = \frac{c_{pf}/(fc)}{c_p/c} \tag{3}$$

E increases as f decreases, as shown below, but it never becomes infinite, even if all the probe sites are blocked. In fact

$$\lim_{f \to 0} E = \frac{2cp_t}{[p_t + K^{-1}][p_t + c + K^{-1} - ((p_t + c + K^{-1})^2 - 4cp_t)^{1/2}]} \tag{4}$$

Usually, not all probe sites can be blocked by ligand because of the sequence specificity of the latter.

We now show that the slope dE/df is always negative. If we define $\alpha = p_t + c + K^{-1}$ and $\beta^2 = (p_t + c + K^{-1})^2 - 4cp_t$, then

$$\frac{dE}{df} = \frac{(\alpha - \beta)^{-1}}{f^2}\left[-p_t - K^{-1} + \frac{\frac{p_t^2}{f} - cp_t + \frac{2p_t}{Kf} + \frac{c}{K} + \frac{1}{fK^2}}{\left(\left[\frac{p_t}{f} + c + \frac{1}{fK}\right]^2 - 4\frac{cp_t}{f}\right)^{1/2}}\right]$$

This will be negative if

$$\left[p_t + \frac{1}{K}\right]\left(\left[\frac{p_t}{f} + c + \frac{1}{fK}\right]^2 - 4\frac{cp_t}{f}\right)^{1/2} > \left[p_t + \frac{1}{K}\right]\left[\left(p_t + \frac{1}{K}\right)\frac{1}{f} + c\right] - 2cp_t \tag{5}$$

To show this, note that $p_t/(p_t + K^{-1}) < 1$, so that

$$0 > \frac{-4c^2p_t}{p_t + K^{-1}} + \frac{4c^2p_t^2}{(p_t + K^{-1})^2}$$

and

$$\left[\frac{p_t}{f} + c + \frac{1}{fK}\right]^2 - \frac{4cp_t}{f} > \left[\frac{p_t}{f} + c + \frac{1}{fK}\right]^2 - \frac{4cp_t}{p_t + K^{-1}}\left[\frac{p_t}{f} + \frac{1}{fK} + c\right] + \left[\frac{2cp_t}{p_t + K^{-1}}\right]^2$$

Therefore

$$\left(\left[\frac{p_t}{f} + c + \frac{1}{fK}\right]^2 - \frac{4cp_t}{f}\right)^{1/2} > \left[p_t + \frac{1}{K}\right]\frac{1}{f} + c - \frac{2cp_t}{p_t + K^{-1}}$$

which probes eq 5, so dE/df is always negative. Therefore, the enhancement E increases monotonically from 1 to $E(0)$ (eq 4), as f goes from 1 to 0, where $1 - f$ is the fraction of sites blocked by the drug.

It is of interest to consider the behavior of E near $f = 1$, by examining the first few terms in the power series in $1 - f$: $E = 1 + c_1(1 - f) + c_2(1 - f)^2 + \ldots$. The first-order coefficient is

$$c_1 = 1 + \frac{c}{\alpha - \beta}\left[-1 + \frac{c + K^{-1} - p_t}{\beta}\right]$$

Similarly, the second-order coefficient is

$$c_2 = 1 + \frac{c}{\alpha - \beta}\left[-1 + \frac{c + K^{-1} - p_t}{\beta}\right] + \frac{c^2(-2p_tK^{-1})}{\beta^3(\alpha - \beta)}$$

Higher coefficients all have a similar form, 1 plus terms in p_t and K^{-1}. If K^{-1} is large compared to c and p_t, these terms are negligible and E becomes $1 + (1 - f) + (1 - f)^2 + \ldots$ or $E = f^{-1}$.

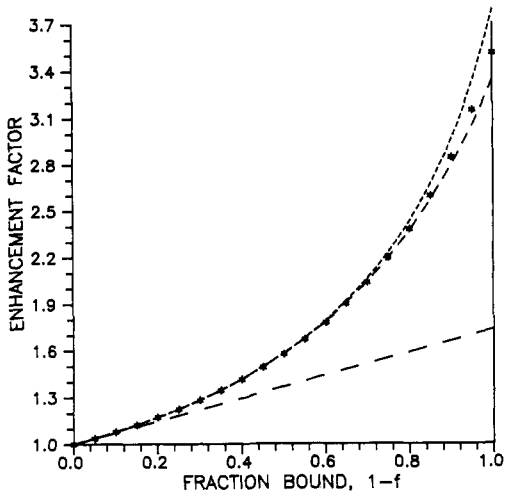

FIGURE 4: Enhancement calculated from a model (see eqs 2–5) in which all probe-binding sites have the same equilibrium constant, $K = 1.5 \times 10^6$ M^{-1}. The total site concentration is $c = 2$ μM and the total probe concentration is $p_t = 0.1$ μM. Points show the enhancement factor E as a function of $1 - f$, the fraction of the probe sites blocked by bound ligand. The dashed straight line is the function $E = 1 + x$ where x is $k(1 - f)$ and k is the initial slope of E. The top curve is $E = (1 - x)^{-1}$. The middle curve is $E = \sum_{i=0}^{6} x^i$.

Characteristics of Mass-Action Enhancement. The points in Figure 4 show the enhancement E as a function of f, calculated according to eq 3, as well as various approximations to it (dashed lines). The parameters used for this example were $p_t = 1 \times 10^{-7}$ M, $c = 2 \times 10^{-6}$ M, $K = 1.5 \times 10^6$ M^{-1}, giving a maximum enhancement $E(0)$ of 3.5. Calculating k as the initial slope of our enhancement factor, $-dE/df$ for $f = 1$, and putting $X = k(1 - f)$, we have plotted $1/(1 - X)$ vs f, obtaining the top curve in Figure 4. It is seen to fit the actual enhancement well for f near 1 but to increase too rapidly for f smaller than about 0.3; it cannot be correct for small f since it incorrectly becomes infinite when $1 - f = k^{-1}$.

Functions which behave like $1/(1 - X)$ for f near 1 but drop below it as f decreases are the power series, $\sum_{i=0}^{n} X^i$ with n finite. The simplest such function is the linear function $1 + X$ ($n = 1$), plotted in Figure 4 as the bottom curve. It is seen that $1 + X$ is a much poorer approximation to the exact E than is $1/(1 - X)$, as is in fact found in the actual calculations on actinomycin (Goodisman et al., 1992). However, one can get a good approximation to E by using a higher value of n. The middle curve in Figure 4, for $n = 6$, tracks the points well for the full range of f.

In our actinomycin calculation (Goodisman et al., 1992), we write the enhancement factor as $E = (1 - K_e c_b)^{-1}$ or as a finite power series, $\sum_{j=0}^{n} (K_e c_b)^j$, where c_b is the concentration of bound ligand and K_e is the enhancement coefficient, whose value is chosen to minimize D. Note that all footprinting plots, for inhibition (binding) sites as well as for enhancement sites, include the effect of enhancement. In inhibitions, E is multiplied by a decreasing function of ligand concentration which depends on the ligand binding constant, and so gives different plots for different sites. All the footprinting plots which do not show the effect of ligand binding, however, are simply multiples of E. If all can be fit by the same function, within a multiplying constant, it is suggested that one is observing a mass-action enhancement.

The value of K_e may be estimated a priori. If c is the concentration of probe-binding sites, and if one bound ligand blocks n of these, $1 - f$ should be nc_b/c, so K_e should be n/c. For actinomycin, which blocks seven sites from DNA cleavage, $K_e = 7 \times 10^6$ M^{-1} since the concentration of probe sites is 1 μM. This is close to what we found (Goodisman et al., 1992) by minimization of D, which confirms that the mass-action effect is mainly responsible for the enhancements observed.

If the fraction of sites blocked by drug, $1 - f$, is not large compared to unity, i.e., for small ligand concentrations, the mass-action enhancement is f^{-1} for all cutting sites. Whether this is in fact true can be ascertained by calculating the "initial relative slopes" of the footprinting plots for enhancement sites (Ward et al., 1988). This is done by fitting the intensities for the lowest ligand concentrations to a linear function of ligand concentration D_t, given by

$$I_j(D_t) = a_j + b_j D_t \quad (6)$$

where j indexes the cleavage site. The initial relative slope is b_j/a_j and should be negative for sites showing inhibition due to ligand binding and positive for enhancement sites and for weak ligand-binding sites, if the ligand concentrations used for the initial relative slopes are not sufficiently high to give appreciable binding at such sites. Note that, to get the magnitude of K_e from slopes, one requires a plot of I_j vs bound-drug concentration c_b, and calculation of c_b requires a knowledge of drug-binding constants. However, for small total drug concentration D_t, the free-drug and bound-drug concentrations are linear in D_t.

For enhancement sites, the initial relative slope should be $K_e c_b/D_t$, since c_b is linear in D_t. This means it should be the same for all sites. Initial relative slopes have been calculated for this experiment, with the standard deviations obtained from the scatter in the footprinting intensities (Ward et al., 1988). The slopes were statistically the same, except for sites immediately adjacent to drug-binding sites, for which they were much larger. This was ascribed to an attractive drug–probe interaction or a distortion of DNA.

Other authors (Low et al., 1984, 1986) have plotted the quantity $F_j = \ln [I_j(D_t)/I_j(0)]$ vs site number j, using the results of only two footprinting experiments, one in the presence of drug at concentration D_t and one in the absence of drug. In these experiments, D_t was large enough so that binding sites were essentially saturated with drug. $F_j > 0$ is an enhancement and $F_j < 0$ shows the effect of drug binding, allowing enhancement sites to be identified from a plot of F_j vs j. A problem with this approach is that no estimate of the uncertainty of F_j is obtained, as one gets from relative initial slope plots, so it is not clear whether F_j is really different for different sites. Furthermore, without footprinting plots (I_j vs D_t for several values of D_t), one cannot know whether all sites with $F_j > 0$ are enhancement sites or whether some are also affected by weak binding. The presence of weak ligand sites would cause certain F_j to be smaller than others (but still positive) and the fact that F_j depends on j would then not imply structural changes. The effect of weak binding is seen in the 139-mer footprinting plots for sites 143 and 145, shown in Figure 3. Similarly, sites 54–58 all show increased cutting with added drug, but it is evident from data for drug concentrations above 20 μM that 54 and 55 are affected by a weak binding site, whereas the others may truly be enhancements. Of course, values of F_j significantly higher than what can be explained by mass action do imply that a structural change is present in addition to the mass-action enhancement.

ANALYSIS

Small Oligomers. For small oligomers with a single ligand-binding site, the analysis of footprinting plots is greatly simplified (Rehfuss et al., 1990a) because a single ligand-binding equilibrium relates the free-drug and bound-drug concentrations to D_t:

$$K = \frac{c_b}{(D_t - c_b)(c - c_b)} \quad (7)$$

Here, $D_t - c_b$ is the free-drug concentration and c is the total concentration of ligand-binding sites, which is also the concentration of oligomers. Furthermore, K_e can be calculated directly. Suppose that there are s cutting sites on the oligomer and that a single bound ligand blocks m of these. Then $1 - f = mc_b/sc$ and the enhancement factor is $E = (1 - mc_b/sc)^{-1} = (1 - K_e c_b)^{-1}$, or $K_e = m/sc$. Since the maximum concentration of bound ligand possible is c, the maximum enhancement is then somewhere between $1 + K_e c = 1 + m/s$ and $(1 - K_e c)^{-1} = (1 - m/s)^{-1}$. It is likely closer to the latter, since $E = (1 - K_e c_b)^{-1}$ tends to overestimate the enhancement slightly and $E = 1 + K_e c_b$ tends to underestimate it (Figure 4).

For example, for DNase I footprinting experiments, actinomycin D is known to block seven sites from cleavage ($m = 7$), four from the size of actinomycin D on DNA, and three sites due to an amino acid "loop" on the enzyme (Suck et al., 1988). For a DNA n-mer, there are $n - 3$ bonds at which cleavage can take place, since DNase I cannot cut at the last three or four bonds at the 3′-ends of the duplex (Lomonosoff et al., 1981; Suck et al., 1988), so $s = n - 3$. Then, for a dodecamer ($n = 12$), the maximum enhancement is $(1 - {}^7/_9)^{-1} = 4.5$. For a 16-mer, one gets a maximum enhancement of $(1 - {}^7/_{13})^{-1} = 2.2$, and for a 20-mer $(1 - {}^7/_{17})^{-1} = 1.70$.

Lane et al. (1987) performed footprinting experiments for the duplexes $d[(AT)_nAGCT(AT)_n]_2$ with $n = 2$, 3, and 4, corresponding to the three cases of the preceding paragraph. The drug was actinomycin D, and the cleavage agent was DNase I. On the 12-mer, inhibited cleavage due to drug binding occurred at all observed sites but one, for which enhanced cleavage was in evidence. NMR measurements showed that the drug binds near the GC and not at the ends of the duplex, where the enhancements occurred. For the 20-mer ($n = 4$), cleavage enhancements, smaller in size than those for the 12-mer, were reported at unblocked sites. Enhancements for the 16-mer were intermediate between those for the other duplexes. It was also noted that the ratio of the ApT cleavage rate to the TpA cleavage rate increased with n. The carrier DNA, which determines the probe concentration, was the same in all the experiments. Therefore, the cleavage rate enhancements in this case and in others (Huang et al., 1988) cannot be explained by the mass-action model. Note that when the probe concentration is large, the mass-action enhancement is small (if $P_t \gg K^{-1}$ and $P_t > c$, eq 4 shows that E is always about 1). Thus, it is likely that the rate increases observed by Lane et al. (1987) are structural in origin.

Multisite DNA. Portugal (1989) studied enhancement of DNase I cleavage by netropsin binding to the Tyr-T DNA fragment, attempting to separate out the effects of the three mechanisms: mass-action, structural changes, and ligand–probe interactions. Netropsin is a minor groove ligand which does not greatly distort DNA upon binding (Kopka et al., 1985). It was reported that 70–71% of the variance of the measured cleavage enhancements could be explained by any of the three mechanisms. Combinations of any two, or of all three, likewise explained 70–71% of the variance. This suggests that a large fraction of the variance simply arises from fluctuations or experimental errors in the measured enhancements. However, since only values of F_j (logarithm of the ratio of cleavage at bond j in the presence of drug to cleavage in the absence of drug) are given, one has no measure of experimental error in these experiments.

The reported values of F_j are plotted against bond number. The average of the 28 F_j values which are positive is 0.75, corresponding to a maximum enhancement of 2.1. Since there are 47 bonds in this fragment and three netropsin sites, each of which blocks about 8 bonds from cleavage, and assuming that the three end bonds cannot be cleaved by DNase I, the maximum enhancement according to the mass-action model is $(1 - {}^{24}/_{44})^{-1} = 2.2$. Thus, the average enhancement observed is consistent with mass action.

Selected footprinting plots (intensity vs total drug concentration) for the actinomycin D–139-mer interaction are shown in Figures 2 and 3, together with the footprinting plots calculated according to our model. By seeking the values of the parameters which minimized the sum of the squared deviations between experimental intensities and those calculated from the model, we found values for binding constants and the enhancement constant K_e. The value of K_e, 7.1×10^6 M^{-1}, is consistent with the mass-action model, which predicts, assuming each bound ligand blocks 7 sites and the concentration of cutting sites is 10^{-6} M, a value of 7.0×10^6 M^{-1}. It does not appear that, with the drug concentrations used, one reaches the maximum enhancement, which would be about $(1 - {}^{105}/_{139})^{-1} = 3.7$, since there are about 139 bonds and 15 independent binding sites.

A plot of initial relative slope vs site number for true enhancement sites makes it easy to recognize deviations from constancy, if any. These deviations, which may be positive or negative, may be ascribed to structural changes. For actinomycin D and netropsin binding to the 139-mer, we suggested on this basis (Ward et al., 1988) that there were structural changes adjacent to binding sites. For both drugs, most of the positive slopes were the same size within the standard deviations, and the average level of enhancement could be explained by mass action. Unusually large slopes were observed for netropsin at sites 52, 53, 64, and 68; binding sites are found at 46–50 (5′-AAATA-3′) and at 56–62 (5′-AATTTAA-3′). For actinomycin, unusually large enhancements were noted for sites 58 and 73, and actinomycin-binding sites of sequence 5′-XGCX-3′ are found at 5′-63–66-3′ and 5′-68–71-3′ (Figure 1).

Obviously, the calculated plots for enhancement sites cannot fit the experimental intensity data in detail, but only on the average, because of the scatter in the experimental points. However, when regular patterns appear in the deviations, they may indicate real effects which our model cannot take into account, such as structural changes. In the case of actinomycin D, one such pattern occurs at very low total drug concentrations, and another occurs at a total drug concentration of about 20 μM.

Figure 2 shows experimental intensities for a number of sites for drug concentrations below 7 μM. The small decrease and increase at about 2 μM is evident on some of these. If this effect is actually due to a structural change induced by drug binding, we may ask which drug-binding events are involved. For small drug concentration, the equilibrium that determines the free-drug concentration D_0 in terms of the total drug concentration D_t is

$$K_c = \frac{D_t - D_0}{D_0[c - (D_t - D_0)]} \quad (8)$$

where K_c is the strong-site binding constant on the carrier and c is the concentration of these sites. Using the values determined by minimization of D, $K_c = 1.8 \times 10^7$ M^{-1} and $c = 5$ μM, a total drug concentration D_t of 2 μM corresponds to a free-drug concentration of 3.6×10^{-8} M. For a site j on the fragment with binding constant K_j, the probability p_j that a drug is bound is determined by the equilibrium

$$K_j = p_j/[D_0(1 - p_j)] \quad (9)$$

so $p_j = D_0K_j/(1 + D_0K_j)$. The two strongest binding sites on the polymer have the sequence 5′-TGCT-3′ and are found at positions 62–65 and 136–139. The determined binding constants were 3.5 and 6.4 μM^{-1}, respectively (Goodisman et al., 1992). Then, with $D_0 = 3.6 \times 10^{-8}$ M and $K_j = 6.4 \times 10^6$ M^{-1}, $p_j = 0.19$; with $K_j = 3.5 \times 10^6$ M^{-1}, $p_j = 0.11$. Other sites are hardly loading drugs at these concentrations. Further, the intensity pattern is evident on almost all footprinting plots from 52 to 103, and apparently it is not present near the strongest binding site. Thus, the structural change in DNA would have to start some 30 base pairs away from the drug and extend some 50 base pairs further. These factors suggest that this pattern should not be ascribed to a structural change.

The other pattern, for 16–24 μM drug, is a sharp intensity decrease for binding-type plots and a sharp increase for enhancement-type plots. The effect is found all over the fragment. This suggests that an abrupt increase in drug binding is occurring at certain sites, producing an abrupt increase in the effective concentration of DNase I, and hence an increase in cutting, at unblocked sites.

At a drug concentration of 20 μM, many sites have appreciable drug loading. Equation 8 is not adequate to calculate D_0, because the weak sites on the carrier become important in determining the free-drug concentration. Our calculations (Goodisman et al., 1992) show that when D_t = 17.2, 20.3, 23.8 μM, D_0 = 3.5, 5.4, and 8.0 μM, respectively. According to eq 9, if $K_j = 2 \times 10^5$ M^{-1}, $p_j = 0.41$ at $D_0 = 3.5$ μM. Thus, all sites with binding constants greater than or equal to 2×10^5 M^{-1} have appreciable drug loading. Thirteen such sites were identified in our study, and there are probably three others outside the part of the fragment measured in our footprinting experiments. Since binding sites are distributed all over the fragment, except in the regions 45–60 and 85–100, it is not surprising that the abrupt intensity changes occur for essentially all cutting sites.

This drug-induced structural change, if that is what is occurring, causes a *decrease* in cutting by enzyme near drug-binding sites and an *increase* at other positions. This suggests that it is associated with increased drug binding, which we referred to previously as positive cooperativity. In our previous work (Goodisman et al., 1992), we therefore modeled the effect as an increase in all binding constants with the amount of drug bound. This mechanism for such cooperative binding could well be a change in the structure of the DNA fragment, acting to increase drug binding rather than to increase cleavage.

Discussion

The local structure of DNA affects the cutting efficiency of DNase I (Drew & Travers, 1984). Intercalating ligands would appear to be the most likely to produce structural changes in DNA which can affect cleavage rates by DNase I or other probes, but groove-binding ligands may also produce such changes (Portugal, 1989). Suck et al. (1988) suggest that the strength of binding, and hence the cutting rate, of DNase I at a site depends mainly on the local minor groove width, which is large in regions rich in GC and small in regions rich in AT. Both kinds of regions then have reduced cutting compared to random sequence DNA. Bending and torsional stiffness also have an effect on the cutting by DNase I (Hogan et al., 1989).

Actinomycin D, though it dimerizes in solution, binds as a monomer, intercalating in DNA at a site that almost always contains a G (Krugh et al., 1977; Rill et al., 1989). The formation of the actinomycin–DNA complex is entropy-driven, and stacking forces are more important than hydrogen bonding (Chiao & Krugh, 1977). It seems reasonable that the binding of actinomycin D alters the structure of the polymer. Netropsin should disturb polymer structure less on binding (Kopka et al., 1985), but it leads to cleavage enhancements similar to actinomycin D in a footprinting experiment (Ward et al., 1988; Fox & Waring, 1984). Furthermore, the size of most of the enhancements is consistent with the mass-action model. This suggests that, rather than interpreting cleavage enhancements as evidence of structural change, one should first consider the mass-action model and then interpret what this model leaves unexplained as due to structural or other changes.

In addition to mass-action and structural changes, an attractive interaction between bound ligand and cleavage agent is a possible cause of enhanced binding (Low et al., 1984; Rehfuss et al., 1990b; Ward et al., 1988). The larger increase in DNase I cleavage at bonds near actinomycin D binding sites may be due to this effect. However, similar increases occur when the porphyrin Mn-T4 is used as a cleavage agent (Rehfuss et al., 1990b). Large enhancements in cleavage by this agent on the 139-mer were observed at sites 60 (near the Act-D binding site at 62–65) and 95 (near the two sites at 100–105). In view of the dramatically different structures of Mn-T4 and DNase I, a ligand–cleavage agent interaction is probably not the correct explanation.

We have considered two possible structural changes on the 139-mer by comparing measured footprinting plots for a large number of sites with plots calculated from a model (Goodisman et al., 1992) in which values for binding constants and other parameters are chosen to give the best possible agreement with experiment. One effect, the large and rapid changes in cutting intensity for total drug concentrations between 16 and 24 μM (free-drug concentrations calculated to be 3.5–8.0 μM), is apparently delocalized over the entire fragment. For these drug concentrations, about 16 drug-binding sites, distributed over almost the entire length of the fragment, are appreciably loaded. Perhaps a major change in polymer structure occurs, leading to a large increase in drug binding at the binding sites and, by way of the mass-action effect, an increase in cutting at sites not blocked by drug.

The other possible structural change occurs for a total drug concentration near 2 μM (free-drug concentration calculated as 0.04 μM). Since the strongest sites are at 62–65 and 136–139, and the intensity pattern seems to be present for all sites up to about 93 and absent for sites with higher numbers, it seems unlikely that this is actually a structural change. Its origin is unknown.

For small oligomers, one normally has only a single ligand-binding site and only a very few footprinting plots showing enhancements. With so few enhancement sites, one cannot use the constancy of the enhancements as evidence for the mass-action effect, although noticeable deviations from constancy do indicate that other effects are operating. However, it is easy to calculate what the mass-action enhancement should be, simply by counting the sites. Deviations from predicted mass-action enhancements, which may be positive or negative in sign, may be ascribed to structural changes indicated by drug binding. On longer fragments, negative deviations from constant mass-action enhancement may be due to the existence of weak binding sites. In this case, smaller increases in cutting rate with drug concentration should occur for groups of contiguous bonds, corresponding to the size of the drug's inhibition region.

Enhancements and Other Probes. In addition to DNase I, the aforementioned mass-action effects are applicable to other

footprinting probes such as Fe–MPE (Dervan, 1986; Dabrowiak et al., 1989a), the porphyrin Mn-T4 (Dabrowiak et al., 1989b), and various metal complexes incorporating *o*-phenanthroline as a ligand (Kuwabara et al., 1986; Uchida et al., 1989). Since these probes must bind in order to cleave DNA, at low probe to DNA ratios their effective concentration at all non-ligand-binding sites *increases* when ligand is added to the system. The observed rate increases would be subject to the same analysis as for DNase I.

The case for the alkylating agents dimethyl sulfate (DMS) and diethyl pyrocarbonate (DEPC), often used as probes in footprinting experiments (Ephrussi et al., 1985; Portugal et al., 1988; Jeppesen & Nielsen, 1988), is less certain. If these agents bind to DNA, they too will exhibit mass-action effects in the footprinting experiment.

Conclusions

In this report we show how to analyze DNase I footprinting data for protein- and drug-induced structural changes in DNA. Since the ligand and DNase I are in equilibrium with DNA, varying the concentration of ligand affects the amount of DNase I bound to DNA. This is because ligand binding to DNA blocks access of the enzyme to certain sites, thereby causing the effective concentration of the enzyme to *increase* at all non-ligand-binding sites. This mass-action effect, resulting in an *increase* in the cleavage rate, must occur with all probes which exist in an equilibrium with DNA. The enhancement of rate is appreciable when the probe concentration is small.

A ligand-induced structural change in DNA can cause a change, *positive* or *negative*, in the cleavage rate constant near the ligand site. The mass-action effect leads to a positive change in the amount of cleavage, which should be equally strong all over the DNA. In order to identify structural changes, it is first necessary to account for the rate enhancement due to mass action. Then one may note those sites having cleavage rates *above* or *below* the values expected for redistribution of the probe molecules on DNA.

Registry No. Actinomycin D, 50-76-0.

References

Chiao, Y.-C. C., & Krugh, T. R. (1977) *Biochemistry 16*, 747–755.

Dabrowiak, J. C., & Goodisman, J. (1989) in *Chemistry and Physics of DNA–Ligand Interactions* (Kallenbach, N. R., Ed.) pp 143–174, Adenine Press, Guilderland, NY.

Dabrowiak, J. C., Kissinger, K., & Goodisman, J. (1989a) *Electrophoresis 10*, 404–412.

Dabrowiak, J. C., Goodisman, J., & Ward, B. (1989b) *Biochemistry 28*, 3314–3322.

Dabrowiak, J. C., Stankus, A., & Goodisman, J. (1991) in *Nucleic Acid Targeted Drug Design* (Propst, C., & Perum, T., Eds.) Marcel Dekker, Inc., New York, NY (in press).

Dervan, P. B. (1986) *Science 232*, 464–471.

Drew, H. R. (1984) *J. Mol. Biol. 176*, 535–557.

Drew, H. R., & Travers, A. A. (1984) *Cell 37*, 491–502.

Ephrussi, A., Church, G. M., Tonegawa, S., & Gilbert, W. (1985) *Science 227*, 134–140.

Fox, K. R., & Waring, M. J. (1984) *Nucleic Acids Res. 12*, 9271–9285.

Goodisman, J., Rehfuss, R., Ward, B., & Dabrowiak, J. C. (1992) *Biochemistry* (preceding paper in this issue).

Hogan, M. E., Robertson, M. W., & Austin, R. H. (1989) *Proc. Natl. Acad. Sci. U.S.A. 86*, 9273–9277.

Huang, Y.-Q., Rehfuss, R. P., LaPlante, S. R., Boudreau, E., Borer, P. N., & Lane, M. J. (1988) *Nucleic Acids Res. 16*, 11125–11139.

Jeppesen, C., & Nielsen, P. E. (1988) *FEBS Lett. 231*, 172–176.

Kopka, M. J., Yoon, C., Goodsell, D., Pujura, P., & Dickerson, R. E. (1985) *Proc. Natl. Acad. Sci. U.S.A. 82*, 1376–1380.

Krugh, T. R., Mosberry, E. S., & Chiao, Y.-C. C. (1977) *Biochemistry 16*, 740–747.

Kuwabara, M., Yoon, C., Goyne, T., Thederahn, T., & Sigman, D. S. (1986) *Biochemistry 25*, 7401–7408.

Lane, M. J., LaPlante, S., Rehfuss, R. P., Borer, P. N., & Cantor, C. R. (1987) *Nucleic Acids Res. 15*, 839–852.

Lomonosoff, G. P., Butler, P. J., & Klug, A. (1981) *J. Mol. Biol. 149*, 745–760.

Low, C. W. L., Drew, H. R., & Waring, M. J. (1984) *Nucleic Acids Res. 12*, 4865–4879.

Low, C. W. L., Drew, H. R., & Waring, M. J. (1986) *Nucleic Acids Res. 14*, 6785–6801.

Portugal, J. (1989) *FEBS Lett. 251*, 8–12.

Portugal, J., Fox, K. R., McLean, M. J., Richenberg, J. L., & Waring, M. J. (1988) *Nucleic Acids Res. 16*, 3655–3670.

Rehfuss, R., Goodisman, J., & Dabrowiak, J. C. (1990a) *Biochemistry 29*, 777–781.

Rehfuss, R., Goodisman, J., & Dabrowiak, J. C. (1990b) in *Molecular Basis of Specificity in Nucleic Acid–Drug Interactions* (Jortner, J., & Pullman, B., Eds.) pp 157–166, Kluwer Academic Publ., Amsterdam.

Rill, R. L., Marsch, G. A., & Graves, D. E. (1989) *J. Biomol. Struct. Dyn. 7*, 591–605.

Suck, D., Lahm, A., & Oefner, C. (1988) *Nature 382*, 465–468.

Uchida, K., Pyle, A. M., Morii, T., & Barton, J. K. (1989) *Nucleic Acids Res. 24*, 10259–10279.

Ward, B., Rehfuss, R., Goodisman, J., & Dabrowiak, J. C. (1988) *Nucleic Acids Res. 16*, 1359–1369.